Formation of Ionic Co-crystals of Amphoteric Azoles Directed by the Ionic Liquid Co-former 1-Ethyl-3-methylimidazolium acetate

Hatem M. Titi,[a] Steven P. Kelley,[a] Max E. Easton,[a] Stephen D. Emerson,[b] and Robin D. Rogers[a,b,c,*]

[a]Department of Chemistry, McGill University, 801 Sherbrooke St. West, Montreal, QC H3A 0B8, Canada

[b]Department of Chemistry, The University of Alabama, Tuscaloosa, AL 35487, USA

[c]525 Solutions, Inc., 720 2nd Street, Tuscaloosa, AL 35401, USA

Contents

1. Materials and Methods.....S1
2. Additional Synthetic and Structural Details S2
2.1. Compound 1 .....S2
2.2. Compound 2 .....S3
2.3. Compound 3 .....S4
2.4. Compound 4 .....S5
2.5. Long term stability.....S6
3. Differential Scanning Calorimetry.....S6
4. Qualitative pK_a Measurement.....S7
5. References……...S9

1. Materials and Methods

3,5-diaminotriazole (DAtz, Sigma Aldrich, St. Louis, MO, USA), 2-methyl-4(5)-nitroimidazole (HmNim, Sigma Aldrich), 4,5-dicyanoimidazole (HDCNim, Alfa Aesar, Ward Hill, MA, USA), 1-ethyl-3-methylimidazolium acetate ([C_2mim][OAc], Iolitec, Tuscaloosa, AL, USA) were used as received. The synthesis of 4,5-di(amidoximyl)imidazole (DAOim) was reported previously.[1]

Single crystal X-ray diffraction (SCXRD) data for **1** ([C_2mim][OAc]·DAtz), **3** ([C_2mim][DCNim]·HDCNim), and **4** ([C_2mim][mNim]·2HmNim) were collected on a Bruker D8 Advance diffractometer (Bruker-AXS, Madison, WI, USA) with a Photon 100 CMOS area detector and an IμS microfocus X-ray source (Bruker AXS) using Mo-Kα radiation. Crystals were coated with Paratone oil (Hampton Research, Aliso Viejo, CA, USA) and cooled to 100 K under a cold stream of nitrogen using an Oxford Cryostream cryostat (Oxford Cryosystems, Oxford, UK). SCXRD data for **2** ([C_2mim][OAc]·DAOim) was collected on a Bruker diffractometer equipped with a PLATFORM 3-circle goniometer and an Apex II CCD area detector (Bruker AXS) using graphite-monochromated Mo-Kα radiation. Hemispheres of data out to a resolution of at least 0.80 Å were collected by a strategy of φ and ω scans. Unit cell determination, data collection, data reduction, and correction for absorption were all conducted using the Apex2 software suite (Bruker AXS). Crystal **1**, **3** and **4** were solved by an iterative dual space approach as implemented in SHELXT[2], while crystal **2** was solved by direct methods and refined by full matrix least squares (SHELXTL software package, Bruker AXS).[3] Non-hydrogen atoms were located from the difference map and refined anisotropically. Acidic hydrogen atoms bonded to

nitrogen and oxygen were located from the difference map and refined as a free variable, while hydrogen atoms bonded to carbon atoms were placed in calculated positions. All hydrogen atom coordinates and thermal parameters were constrained to ride on the carrier atoms. Anomalous thermal ellipsoids for some of the carbon atoms on the $[C_2mim]^+$ cation were found in **2**, possible due to unresolvable disorder, a global restraint was added to keep the components of the thermal tensors of all atoms equal along the axes of covalent bonds.[4]

Differential scanning calorimetry (DSC) was measured on a DSC2500 (TA instruments Ltd., Delaware, USA), under a stream of nitrogen gas. Samples (4-9 mg) were placed in lidded but unsealed aluminum pans. Samples of the liquids (or suspension) were first cooled to -90 °C (the lower limit of our DSC) and then warmed to at least 10 °C above the reported melting point of each azole (215 °C for DAtz; 190 °C for HDCNim and HmNim). DAOim was confirmed visually to decompose on melting and so was warmed only to 175 °C, approximately 20 °C below its $T_{5\%}$ decomposition temperature. All heating and cooling steps were done at a ramp rate of 5 °C/min and followed by an isotherm (5 min. at the end of heating steps, 10 min. at the end of cooling steps). Three consecutive cycles were run for consistency.

Powder X-ray diffraction (PXRD) data was collected on a Bruker D8 Advance equipped with a Lynxeye linear position sensitive detector (Bruker AXS, Madison, WI). Neat samples were smeared directly onto the silicon wafer of a proprietary low-background sample holder. Data was collected using a continuous coupled θ/2θ scan with Ni-filtered Cu-Kα radiation.

2. Synthesis and Crystal Structure Details:

2.1 Compound 1 ($[C_2mim][OAc]\cdot DAtz$):

Additional grinding attempts are presented in **Table S1** and either led to the formation of crystals that were indexed as the starting material DAtz[5] or did not yield crystals.

Table S1: Different molar combinations of DAtz and $[C_2mim][OAc]$

DAtz (mg)	$[C_2mim][OAc]$ (mg)	Mole Ratio (Azole:IL)	Observations
2.0	17.7	1:5	Colorless oil
2.9	16.3	1:3	**Compound 1**
4.0	14.0	1:2	Start material crystals of DAtz
5.6	11.1	1:1.1	
6.1	10.7	1:1	
6.4	9.1	1.2:1	
7.2	8.2	1.5:1	
8.9	5.6	3:1	

SCXRD analysis revealed that the heterocyclic ring of the $[C_2mim]^+$ ion is geometrically planar, and the bond distances match with the known structure of $[C_2mim][Cl]$ (CCDC: VEPFOL01).[6] The ethyl group is tilted with respect to the heterocyclic ring, with a torsion angle (C7-C6-N1-C4) of 51.4° (61.0° in VEPFOL01). The cation and anion are separated from each other by a distance of 3.323(2) Å. This is a

significantly longer separation between ions than the previously reported structure of $[C_2C_2im][OAc]$ (0.2 Å.[7]).

Other weak intermolecular forces are involved in stabilizing the crystal packing between fragments. **Fig. S1** shows the molecular environments of each fragment of **1**. The cation is involved in only weak intermolecular interactions (such as C-H···O and C-H···π), and is surrounded by two neutral azoles and three acetate entities. On the other hand, the anion is surrounded by two acetate moieties forming weak hydrogen-bonding chains through the methyl groups. Three neighboring neutral DAtz azoles are directly bonded through the amine groups via the O-atoms of the acetate. Only one cation was seen to form weak hydrogen bonding with the anion. The neutral DAtz azole is engaged with two additional azole moieties through hydrogen bonds, three acetate groups, and two cations. The acetate ions form hydrogen bonds with the amine groups while the cations are forming weaker intermolecular interactions through C-H···π bonds.

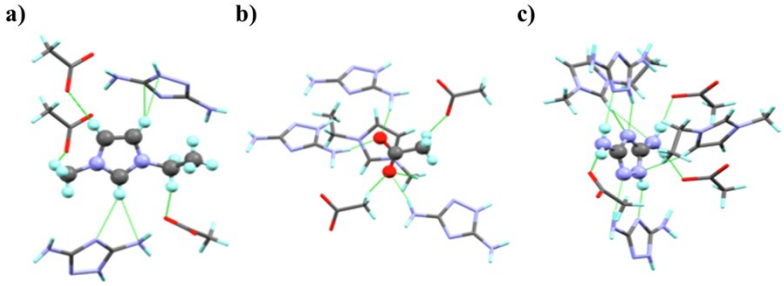

Fig. S1 Short (less than the sum of the van der Waals radii) contact environments of the $[C_2mim]^+$ cation (a), $[OAc]^-$ anion (b), and neutral DAtz (c) in **1**.

2.2 Compound 2 ($[C_2mim][OAc]\cdot$DAOim):

The molecular environment of the $[C_2mim]^+$ cations (**Fig. S2**) are occupied by one anion, one cation, and four DAOim entities through short contacts. In this cation, the ethyl group is significantly tilted out of the plane of the imidazole ring, with a torsion angle of 133.0°.

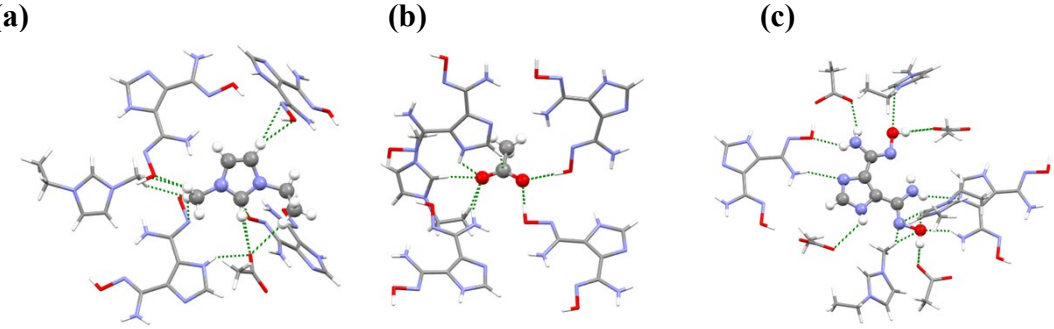

Fig. S2 Short (less than the sum of the van der Waals radii) contact environments of the $[C_2mim]^+$ cation (a), $[OAc]^-$ anion (b), and neutral DAOim (c) in **2**.

The anion is surrounded by four neutral azole molecules and one cation which interact through a series of strong and weak hydrogen bonds. The most crowded environment is that of DAOim, with nine fragments comprising four anions, three cations, and two DAOim entities. The strongest interaction is between the acetate entity and the hydroxyl group of DAOim, with nearly linear contacts of 2.582(5) Å.

2.3 Compound 3 ([C_2mim][DCNim]·HDCNim):

Additional grinding attempts are presented in **Table S2** and either led to the formation of crystals that were indexed as the starting material HDCNIm,[8] or did not yield crystals.

Table S2: Different molar combinations of HDCNim and [C_2mim][OAc]

HDCNim (mg)	[C_2mim][OAc] (mg)	Mole ratio (Azole:IL)	Observations
14.8	43.2	1:2	Oil
20.2	43.0	1:1.5	
25.2	43.1	1:1.2	
29.7	43.1	1:1	
36.1	43.0	1.2:1	**Compound 3**
44.9	43.2	1.5:1	Start material crystals of HDCNim
60.2	43.3	2:1	

The [C_2mim]$^+$ cation is surrounded by two cations, four anions, and one azole through short contacts (**Fig. S3**). The molecular environment surrounding the cation involves all the imidazolium ring acidic hydrogen atoms at C2, C4, and C5. The ethyl group is tilted from the plane of the heterocycle, with a torsion angle of -100.6°. The anion is engaged with four cations and two azoles, while the azole environment occupied by seven fragments: two cations, two anions, and four azoles. The proton assists in the formation of stable and strong N-H···N hydrogen bonds (2.644(2) Å), while the cation is involved in weaker C-H···N hydrogen interactions through the acidic C2 H-atom (as does the H-atom of C5).

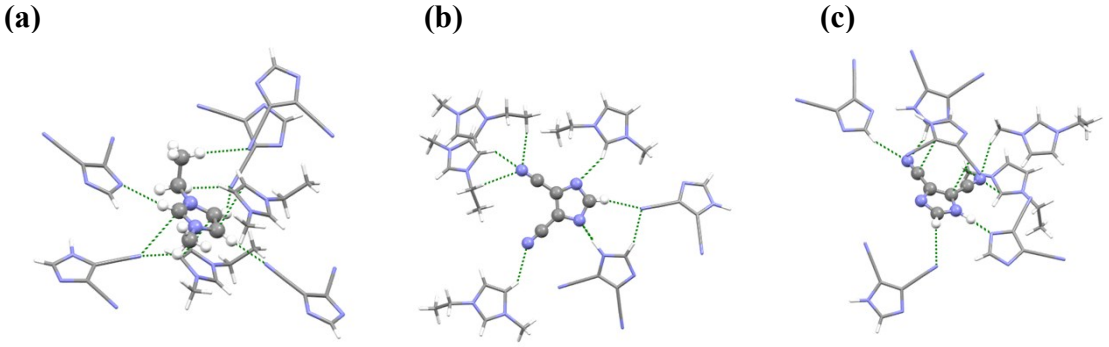

Fig. S3 Short (less than the sum of the van der Waals radii) contact environments of the [C_2mim]$^+$ cation (a), [DCNim]$^-$ anion, (b) and neutral HDCNim (c) in **3**

2.4 Compound 4 ([C_2mim][mNim]·2HmNim):

Additional grinding attempts are presented in **Table S3** and either led to the formation of crystals that were indexed as the starting material HmNim[7] or did not yield crystals.

Table S3: Different molar combinations of HmNim and [C_2mim][OAc]

HmNim (mg)	[C_2mim][OAc] (mg)	Mole Ratio (Azole:IL)	Phase

14.0	75.2	1:4	Yellow oil
23.1	65.3	1:2.1	Yellow oil
33.0	54.1	1:1.2	**Compound 4**
40.2	43.9	1.2:1	Start material crystals of HmNim
45.2	40.7	1.5:1	
49.9	37.1	1.7:1	
52.9	29.4	2.5:1	
68.0	22.1	4:1	

The analysis of the residual electron density maps represented by OLEX2[9] (OlexSys, Durham University, UK) without the attribution of hydrogen atom involved in hydrogen interactions between the mNim azoles. **Fig. S4** confirms the location of the hydrogen atoms on the nitrogen atoms of the terminal azoles, which assisted in assigning the neutral azoles along the oligomeric delocalized anion.

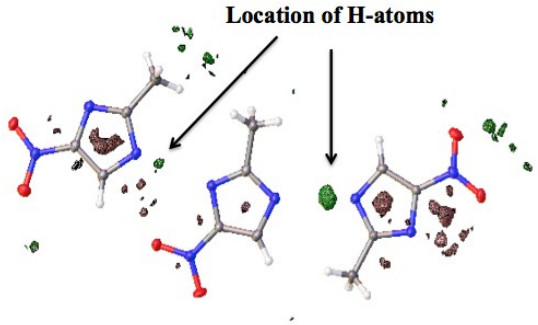

Fig. S4 Electron density maps of the oligomeric delocalized anion of **4** demonstrate that two protons are located near to the 'terminal' mNim azoles (represented by green-wired maps). The fragment pictured in the middle of the oligomer is formally assigned as an anion.

The cation in **4** is surrounded by five neutral azoles and two anions, in which the anions are located above and beneath the cation (**Fig. S5a**). The cation is involved mainly in weak interactions (such as C-H···π and C-H···O/N) with surrounding fragments. Similarly, the anion is located between two cations above and below the azole ring, in addition to three neutral azoles. Two of the neutral azoles form hydrogen-bonding interactions through the hydrogen atoms of the N-donors of the anion, while a third neutral molecule forms weaker interactions through the nitro group. The first neutral mNim azole (**Fig. S5c**) is surrounded by two cations, four neutral mNim azoles and two anions. Two of the neutral components participate in π···π stacking with the azole. The nitro groups are involved in various non-covalent interactions. Interestingly, the molecular environment of the second neutral azole (**Fig. S5d**) is less crowded, with a series of intermolecular interactions linking it to three cations, two neutral azoles, and one anion.

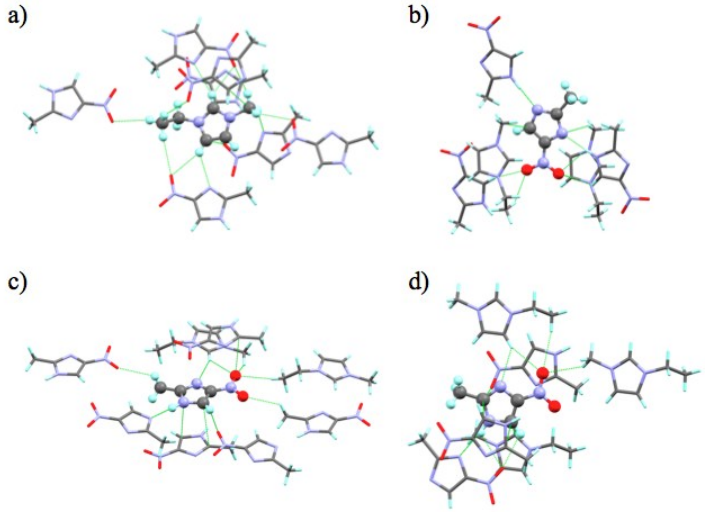

Fig. S5 Short (less than the sum of the van der Waals radii) contact environments of the $[C_2mim]^+$ cation (a), $[mNim]^-$ anion (b), first mNim unit (c), and second mNim unit (d) in **4**.

2.5. Long Term Stability

After *ca.* 1 year in storage, compounds **1-3** were found to have converted completely back to liquids. The reaction mixture from which compound **4** crystallized contained crystals, but PXRD analysis of these indicated that HmNim was the only crystalline phase (**Fig. S6**). Together, these observations reveal that the co-crystals are either themselves deliquescent or able to dissolve in water absorbed by $[C_2mim][OAc]$ over time.

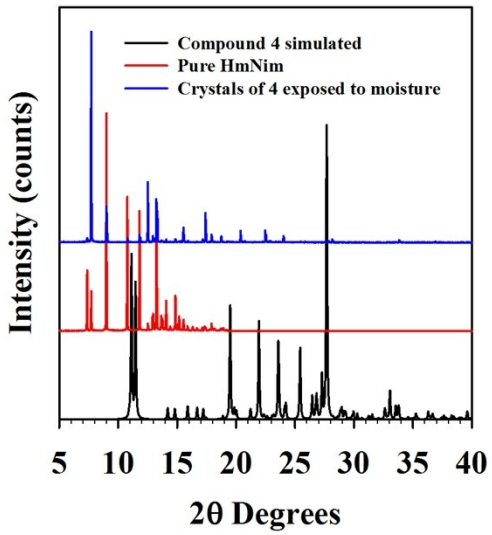

Fig. S6: PXRD patterns of compound **4** after extensive storage compared to the measured PXRD of HmNim and simulated PXRD from the single crystal structure of **4**.

3. Differential Scanning Calorimetry (DSC)

Reaction mixtures of [C_2mim][OAc] and each azole were prepared at the compositions which yielded single crystals of **1-4**, as reported in **Tables S1-S4**. Grinding DAOim with [C_2mim][OAc] gave a liquid with a small amount of suspended powder, while all other azoles gave liquids as observed previously. DSC data are summarized in **Fig. S7**.

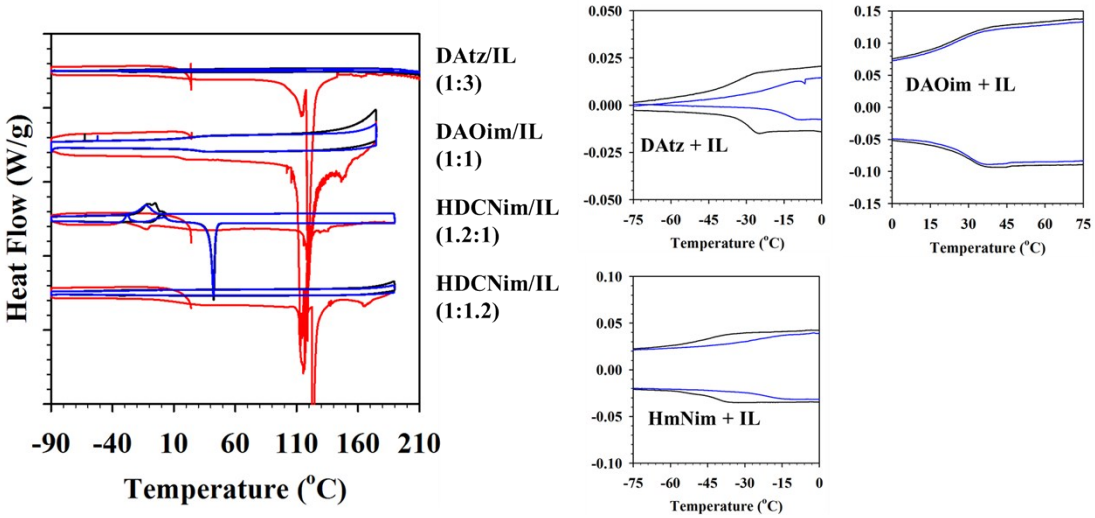

Fig. S7: DSC measurements of combinations of each azole with [C_2mim][OAc] (abbreviated IL). *Left*: Full data for all three cycles of all combinations. Scale for y-axis is 0.2 W/g per each minor tick mark. Ratios on the right axis are mol:mol. Cycles are color coded: Red – 1st cycle, black – 2nd cycle, blue – 3rd cycle. *Right*: Expanded graphs of the glass transition regions.

There were no transitions in any of these samples on first cooling that indicated crystallization of any of the liquids. HDCNim/[C_2mim][OAc] showed a small exothermic transition on first warming (*ca*. -31.1 °C) followed by an endothermic transition (*ca*. -11.7 °C), which might be an incomplete or interrupted crystallization event. All four reaction mixtures then exhibited a major endothermic event near 118 °C, which occurs only on first warming. This has been assigned to the evaporation of acetic acid, as it is an irreversible transition occurring very close to the normal boiling point of acetic acid (118.1 ºC). HmNim/[C_2mim][OAc] shows a very sharp and irreversible endothermic transition immediately following it at 121.57 ºC, which may be an unexpected decomposition of the azolate anion. Of the four reaction mixtures, only HDCNim/[C_2mim][OAc] undergoes reversible crystallization and melting (mp 42.21 ºC). The other reaction mixtures only undergo reversible liquid-glass and glass-liquid transitions on subsequent cycles.

3. Qualitative pKa measurements:

In this study, we investigated the influence of each azole's pKa on the co-crystallization process with [C_2mim][OAc], to determine whether it fit into conventional wisdom regarding pKa and co-crystal formation.[10] We thus aimed to determine whether we were able to control the formation of either co-crystals or salts using [C_2mim][OAc]. Conventional wisdom dictates that the consequence of a reaction between an acid and base can be predicted by the eq. 1:

$$\Delta pKa = pKa_{base} - pKa_{acid} \quad (1)$$

where ΔpKa values greater than 3 predict the formation of a salt, while co-crystals can be obtained from values less than 0. Values between 0 and 3 are not as predictable, and may result in either (or both) regimes.[11]

For our compounds, we utilized a known procedure of qualitative measurement of pKa ranges through the use of a series of indicators (Table S4.)[12] Stock solutions of the indicators were prepared by diluting the solids at a concentration of 0.2 mg/mL in an ethanol:water mixture (1:4 v/v). 0.1 mmol of the tested compound was then added to an aliquot of the stock indicator solution. Changes in color indicated the pK_a values for each compound as described in Table S4, and enabled us to qualitatively determine the acidities.

Table S4 The pKa values of the used indicators and their color change dependence

Indicator	**p*K*$_a$**	**Color**	
		Acid-form	**Base-form**
Methyl Yellow	3.3	Red	Yellow
Methyl Red	4.8	Red	Yellow
Bromothymol Blue	7.2	Yellow	Green
Phenolphthalein	9.3	Colorless	Red
2,4-Dinitroaniline	15.0	Yellow	Violet

The results listed in Table S5 demonstrate the basicity of [C_2mim][OAc], found to have a pKa value above 7.2. The pKa range of DAtz is also in this region. HDCNim exhibits an acidic pKa range of less than 3.3, and is the most acidic azole in this study. Therefore, from eq. 1, we expect that the formation of co-crystals is more likely to progress when using DAtz as the azole component, while salts are more likely to form with the use of DCNim. This prediction from ΔpKa values was confirmed by the formation of the ionic co-crystal of **1**. A reaction between [C_2mim][OAc] and HmNim (which bears structural similarity to HDCNim) is a typical acid-base reaction, where ΔpKa is above 3, and is predicted to form a salt, which indeed occurred in the formation of **4**. The DAOim molecule contains amidoximyl groups, which are expected to show high pKa values owing to the presence of lone pair electrons on the nitrogen and oxygen atoms. Therefore it was expected that DAOim would form a co-crystal on reaction with [C_2mim][OAc], which we observed in crystal structure **2**.

Table S5 The color changes of the studied compounds following exposure to the pKa-determining indicators

Indicators	**HDCNim**	**HmNim**	**DAtz**	**[C_2mim][OAc]**
Methyl Yellow	Red	Yellow	Yellow	Yellow
Methyl Red	Red	Red	Red	Yellow
Bromothymol Blue	Yellow	Yellow	Green	Green

Phenolphthalein	Colorless	Colorless	Colorless	Colorless
2,4-Dinitroaniline	Yellow	Yellow	Yellow	Yellow

4. References

1 S. P. Kelley, P. S. Barber, P. H. Mullins and R. D. Rogers, *Chem. Commun.*, 2014, **50**, 12504-12507.

2 G. M. Sheldrick, *Acta Crystallogr. C Struct. Chem.*, 2015, **71**, 3-8.

3 a) G. M. Sheldrick, *Acta Cryst. Sect. A* 2015, **A71**, 3-8; b) G. M. Sheldrick, *SHELXTL Structure Determination Suite* v.6.10, Bruker-AXS, Inc.; Madison, WI 2010.

4 A. Thorn, B. Dittrich and G. M. Sheldrick, *Acta Cryst. Sect. A Found. Crystallogr.*, 2012, **A68**, 448-451.

5 T. M. Klapötke, F. A.Martin, N. T. Mayr and J. Stierstorfer, *Z. Anorg. Allg. Chem*., 2010, **636**, 2555-2564.

6 S. Parsons, D. Sanders, A. Mount, A. Parsons and R. Johnstone, *CSD Communication* **2006**, 767968.

7 G. Gurau, H. Rodriguez, S. P. Kelley, P. Janiczek, R. S. Kalb and R. D. Rogers, *Angew. Chem. Int. Ed. Engl.*, 2011, **50**, 12024-12026.

8 E. Barni, R. Bianchi, G. Gervasio, A. T. Peters and G. Viscardi*, J. Org. Chem*., 1997, **62**, 7037-7043.

9 O. Dolomanov, L. Bourhis, R. Gildea, J. Howard and H. Puschmann*, J. Appl. Crystallogr*., 2009, **42**, 339-341

10 S. P. Kelley, A. Narita, J. D. Holbrey, K. D. Green, W. M. Reichert and R. D. Rogers, *Cryst. Growth Des.*, 2013, **13**, 965-975.

11 L. Scott, G. Childs, P. Stahly and A. Park, *Molecular Pharmaceutics*, 2007, **4**, 323-338.

12 K. Tanabe, H. Misono, H. Hattori and Y. Ono, *New Solid Acids and Bases*. Elsevier Science: 1989.